Journal of Solid State Chemistry 182 (2009) 55–59

Contents lists available at ScienceDirect

Journal of Solid State Chemistry

journal homepage: www.elsevier.com/locate/jssc

Transition metal tetramolybdate dihydrates $MMo_4O_{13} \cdot 2H_2O$ ($M = Co,Ni$) having a novel pillared layer structure

Kazuo Eda [a,*], Yu Ohshiro [a], Noriko Nagai [a], Noriyuki Sotani [a], M. Stanley Whittingham [b]

[a] Department of Chemistry, Graduate School of Science, Kobe University, Nada-ku, Kobe 657-8501, Japan
[b] Institute for Materials Research, State University of New York at Binghamton, Binghamton, NY 13902-6000, USA

ARTICLE INFO

Article history:
Received 21 August 2008
Received in revised form
30 September 2008
Accepted 2 October 2008
Available online 14 October 2008

Keywords:
Hydrothermal synthesis
Molybdate
Crystal structure
$CoMo_4O_{13} \cdot 2H_2O$
$NiMo_4O_{13} \cdot 2H_2O$

ABSTRACT

Hydrothermal synthesis in the M/Mo/O ($M = Co,Ni$) system was investigated. Novel transition metal tetramolybdate dihydrates $MMo_4O_{13} \cdot 2H_2O$ ($M = Co,Ni$), having an interesting pillared layer structure, were found. The molybdates crystallize in the triclinic system with space group $P{-}1$, $Z = 1$ with unit cell parameters of $a = 5.525(3)$ Å, $b = 7.058(4)$ Å, $c = 7.551(5)$ Å, $\alpha = 90.019(10)^\circ$, $\beta = 105.230(10)^\circ$, $\gamma = 90.286(10)^\circ$ for $CoMo_4O_{13} \cdot 2H_2O$, and $a = 5.508(2)$ Å, $b = 7.017(3)$ Å, $c = 7.533(3)$ Å, $\alpha = 90.152(6)^\circ$, $\beta = 105.216(6)^\circ$, $\gamma = 90.161(6)^\circ$ for $NiMo_4O_{13} \cdot 2H_2O$ The structure is composed of two-dimensional molybdenum-oxide (2D Mo-O) sheets pillared with CoO_6 octahedra. The 2D Mo-O sheet is made up of infinite straight ribbons built up by corner-sharing of four molybdenum octahedra (two MoO_6 and two MoO_5OH_2) sharing edges. These infinite ribbons are similar to the straight ones in triclinic-$K_2Mo_4O_{13}$ having 1D chain structure, but are linked one after another by corner-sharing to form a 2D sheet structure, like the twisted ribbons in $BaMo_4O_{13} \cdot 2H_2O$ (or in orthorhombic-$K_2Mo_4O_{13}$) are.

1. Introduction

Transition metal molybdates are attractive compounds because of their structural, magnetic, and catalytic properties [1–11]. They are especially important components of industrial catalysts. Their catalytic properties are closely related to their structure [7,9]. Thus it is important to develop materials with novel structural features.

As is now well-known, hydrothermal syntheses can lead to the formation of materials at much lower temperatures than those necessary in solid-state syntheses. The lowering of synthetic temperature may allow an access to materials with novel structural features. With the aim of searching novel synthetic routes and materials, we have been investigating reactions under hydrothermal conditions [12–16].

Recently we have studied the hydrothermal reactions of the M/Mo/O ($M = Co,Ni$) system, and then found new transition metal tetramolybdate dihydrates $MMo_4O_{13} \cdot 2H_2O$ ($M = Co,Ni$) that exhibited an interesting pillared layer structure. Here we report the hydrothermal preparation, crystal structure, and some properties of $MMo_4O_{13} \cdot 2H_2O$. Moreover, structural comparison with other known tetramolybdates are described briefly.

2. Experimental

Title compounds were synthesized by a hydrothermal technique. $MCl_2 \cdot 6H_2O$ were used as M sources, while insoluble MoO_3 and soluble $MoO_3 \cdot nH_2O$ were utilized as the Mo source. $MoO_3 \cdot nH_2O$ was prepared according to the procedure mentioned previously [17]. The hydration number n was determined to be around 1.1 by thermogravimetric and differential thermal analyses (TG-DTA). The mixture of the M and Mo sources was dissolved or suspended in 40 mL of water. The resulting solution was put into a 60 mL Teflon-lined autoclave and heated in a forced convection oven at 453 K under autogenous pressure for the desired time. The resulting product was filtered, washed with distilled water, and dried in air at room temperature.

Powder X-ray diffraction of the product was measured on a Mac Science MXP3VZ X-ray diffractometer with a graphite monochromator using Cu$K\alpha$ radiation. Single crystal X-ray diffraction data were collected on a Bruker smart1000 diffractometer with a CCD detector using graphite monochromated Mo$K\alpha$ radiation. The single crystal structure was solved by direct method and refined by full-matrix least-squares calculations based on F_o^2 with empirical absorption corrections using Bruker SHELXTL programs. The composition of the product was determined by a HITACHI 180–80 atomic absorption spectrometer using the 313.3 nm line for Mo, 240.7 nm for Co, and 232.0 nm for Ni. TG-DTA measurements were performed in N_2 on a Mac Science TG-DTA 2010S system at a heating rate of 10 K min^{-1}. FT-IR spectra

* Corresponding author. Fax: +81 78 803 5677.
E-mail address: eda@kobe-u.ac.jp (K. Eda).

0022-4596/$ - see front matter © 2008 Elsevier Inc. All rights reserved.
doi:10.1016/j.jssc.2008.10.001

of the samples were measured on a Perkin-Elmer Spectrum 1000 FT-IR spectrometer using the KBr pellet method.

3. Results and discussion

3.1. Hydrothermal syntheses

We tried to prepare novel transition metal molybdates by a hydrothermal technique. As mentioned above, insoluble MoO_3 and soluble $MoO_3 \cdot nH_2O$ were used as Mo sources. Synthetic parameters used in the present work were summarized in Table 1, together with the products obtained. Several XRD patterns of the resulting solid products were shown in Fig. 1.

In this work novel transition metal molybdate hydrates $MMo_4O_{13} \cdot 2H_2O$ (M = Co,Ni) [18], structural details of which will be described below, and MoO_3 were obtained. $CoMo_4O_{13} \cdot 2H_2O$ and $NiMo_4O_{13} \cdot 2H_2O$ exhibited similar XRD patterns, and were expected to be isostructural with each other. The formation of $MMo_4O_{13} \cdot 2H_2O$ depended on the kinds of Mo and M sources, and the treatment time. Comparison of the results obtained from the soluble Mo source (Runs 4–6) with those from the insoluble Mo source (Runs 1–3) indicated that the usage of the soluble Mo source was effective for the formation of $MMo_4O_{13} \cdot 2H_2O$ (i.e., the usage greatly reduced the treatment time required for the formation). Moreover, we found that large crystals of $MMo_4O_{13} \cdot 2H_2O$ were obtained when the hydrothermal solution was cooled slowly after the hydrothermal treatment, while powder-like $MMo_4O_{13} \cdot 2H_2O$ precipitated when cooled rapidly. This indicates that $MMo_4O_{13} \cdot 2H_2O$ was present as solute (i.e., has considerably high solubility) in the solution during the hydrothermal treatment, but precipitated due to lowering of the solubility during cooling of the solution. In the case of $NiMo_4O_{13} \cdot 2H_2O$, its preparation required the three-day treatment, and the hydrothermal solution treated for one day did not contain enough amount of $NiMo_4O_{13} \cdot 2H_2O$ for precipitation (cf. Runs 8, 9, 11, 12). This may indicate that $MMo_4O_{13} \cdot 2H_2O$ is formed by conversion from other soluble M/Mo/O species in the solution, which species have not been identified. The quantitative yield in the synthetic condition of soluble Mo source, [Mo] = 0.06 M ($\equiv$mol L^{-1}), [M]/[Mo] = 10, and treatment temperature = 453 K was 85% (by weight, based on Mo) for $CoMo_4O_{13} \cdot 2H_2O$ prepared by the one-day treatment, while 21% for $NiMo_4O_{13} \cdot 2H_2O$ by the three-day treatment. For obtaining crystals good for single crystal X-ray diffraction measurements, it is generally effective to prepare products in a small excessive amount over saturation point. Thus $CoMo_4O_{13} \cdot 2H_2O$ crystals suitable for the measurements could be prepared in the condition of [Mo] = 0.02 M.

3.2. Crystal structures of the $MMo_4O_{13} \cdot 2H_2O$

Single crystals used for X-ray diffraction measurements were obtained by cooling the sample solution slowly after the hydrothermal treatment. A dark red needle, dimensions $0.15 \times 0.06 \times 0.04$ mm, of $CoMo_4O_{13} \cdot 2H_2O$ and a pale blue needle, $0.17 \times 0.04 \times 0.02$ mm, of $NiMo_4O_{13} \cdot 2H_2O$ were used for the measurements. The resulting crystallographic and refinement details are summarized in Table 2 [19]. Further details of the crystal structure investigations can be obtained from the Fachinformationszentrum Karlsruhe, 76344 Eggenstein-Leopoldshafen, Germany (fax: (49) 7247 808 666; e-mail: crysdata@fiz.karlsruhe.de) on quoting the CSD numbers given in Table 2.

Initial heavy-atom positions (Mo, Co, Ni) were located using the direct-method, and the oxygen atom positions were located from iterated Fourier difference maps during the refinement.

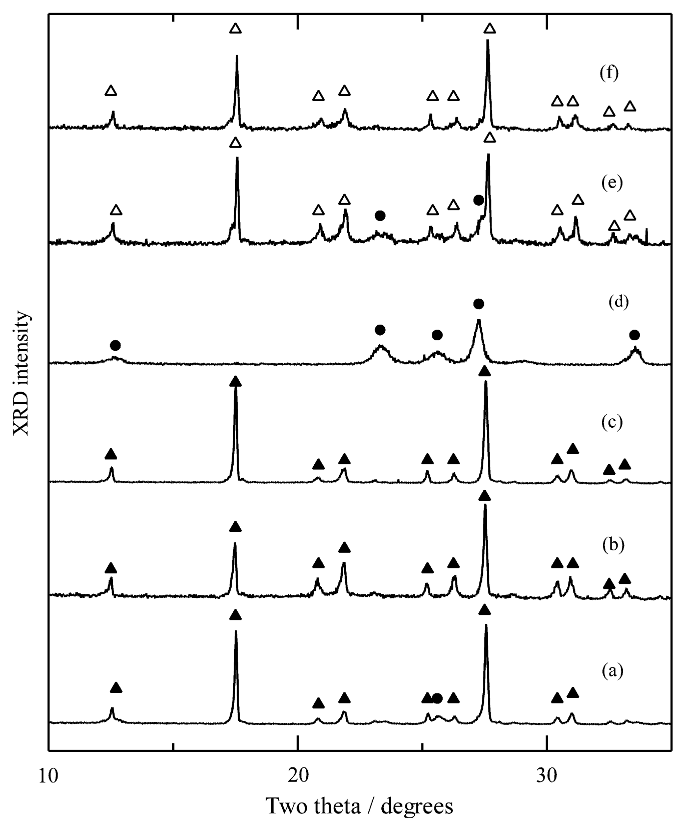

Fig. 1. Powder XRD patterns of the products: run 4 (a), run 5 (b), run 6 (c), run 10 (d), run 11 (e), and run 12 (f). Symbols ●, ▲, Δ indicate MoO_3, $CoMo_4O_{13} \cdot 2H_2O$, $NiMo_4O_{13} \cdot 2H_2O$, respectively.

Table 1
Synthetic conditions and products obtained

Run	Mo source	M source	[M]/[Mo]	pH	Treatment time (days)	Products
1	MoO_3	$CoCl_2 \cdot 6H_2O$	1	3.94	3	$CoMo_4O_{13} \cdot 2H_2O$+MoO_3
2	MoO_3	$CoCl_2 \cdot 6H_2O$	5	3.73	3	$CoMo_4O_{13} \cdot 2H_2O$
3	MoO_3	$CoCl_2 \cdot 6H_2O$	10	3.50	3	$CoMo_4O_{13} \cdot 2H_2O$
4	$MoO_3 \cdot nH_2O$	$CoCl_2 \cdot 6H_2O$	1	1.91	1	$CoMo_4O_{13} \cdot 2H_2O$+MoO_3
5	$MoO_3 \cdot nH_2O$	$CoCl_2 \cdot 6H_2O$	5	1.64	1	$CoMo_4O_{13} \cdot 2H_2O$
6	$MoO_3 \cdot nH_2O$	$CoCl_2 \cdot 6H_2O$	10	1.45	1	$CoMo_4O_{13} \cdot 2H_2O$
7	$MoO_3 \cdot nH_2O$	$NiCl_2 \cdot 6H_2O$	1	1.57	1	MoO_3
8	$MoO_3 \cdot nH_2O$	$NiCl_2 \cdot 6H_2O$	5	1.39	1	No precipitation
9	$MoO_3 \cdot nH_2O$	$NiCl_2 \cdot 6H_2O$	10	1.25	1	No precipitation
10	$MoO_3 \cdot nH_2O$	$NiCl_2 \cdot 6H_2O$	1	1.57	3	MoO_3
11	$MoO_3 \cdot nH_2O$	$NiCl_2 \cdot 6H_2O$	5	1.39	3	$NiMo_4O_{13} \cdot 2H_2O$+MoO_3
12	$MoO_3 \cdot nH_2O$	$NiCl_2 \cdot 6H_2O$	10	1.25	3	$NiMo_4O_{13} \cdot 2H_2O$

Table 2
Crystallographic and refinements details of $MMo_4O_{13}\cdot 2H_2O$

	$CoMo_4O_{13}\cdot 2H_2O$	$NiMo_4O_{13}\cdot 2H_2O$
Crystal system	Triclinic	Triclinic
Space group	$P\bar{1}$ (no. 2)	$P\bar{1}$ (no. 2)
a/Å	5.525 (3)	5.508 (2)
b/Å	7.058 (4)	7.017 (3)
c/Å	7.551 (5)	7.533 (3)
α/°	90.019 (10)	90.152 (6)
β/°	105.230 (10)	105.216 (6)
γ/°	90.286 (10)	90.161 (6)
Cell volume/Å^3	284.1 (3)	280.90 (18)
Z	1	1
R_{int}	0.0335	0.0261
$R_1(F)$ ($I<2\sigma(I)$)	0.0636	0.0619
$wR_2(F^2)$ for all reflection	0.1819	0.1786
Goodness-of-fit	1.086	1.047
CSD no.	419 795	419 794

Table 3
BVS values of atoms in $CoMo_4O_{13}\cdot 2H_2O$

Atoms	BVS
Mo1	6.22
Mo2	6.08
Co1	2.28
O1	2.13
O2	2.09
O3	2.11
O4	1.86
O5	2.02
O6	2.03
O7	2.10
O8	0.30

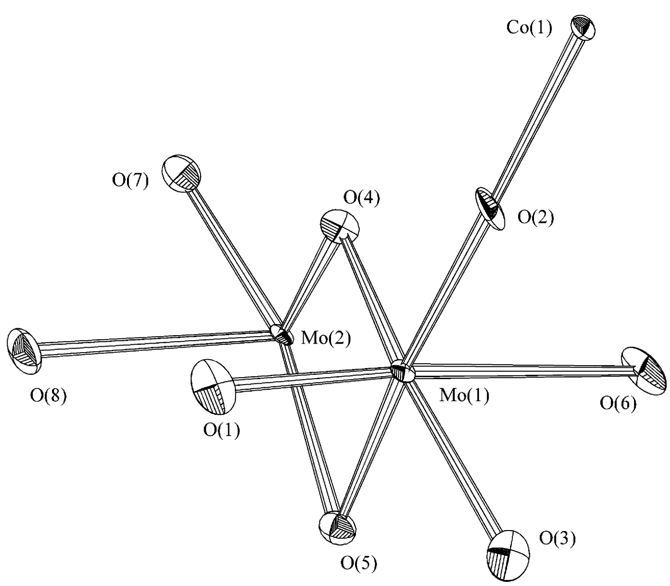

Fig. 2. Asymmetric atomic configuration and atom-labeling in $CoMo_4O_{13}\cdot 2H_2O$. Displacement ellipsoids are drawn at the 50% probability level.

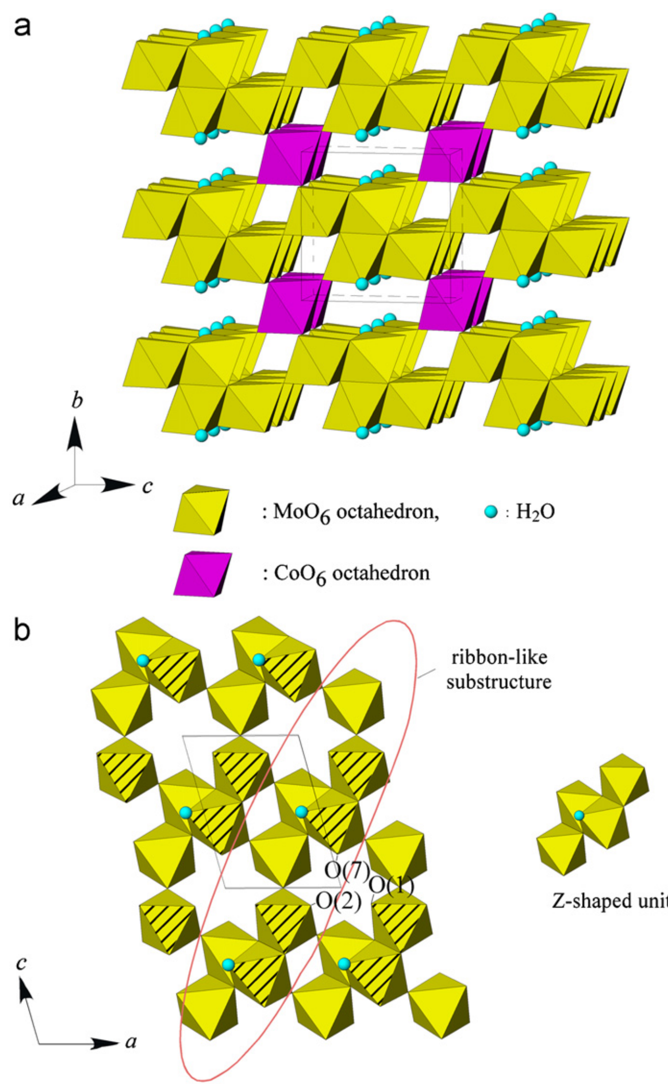

Fig. 3. Crystal structure of $CoMo_4O_{13}\cdot 2H_2O$.

These non-hydrogen atoms were refined anisotropically. No hydrogen postions could be located from the final difference map, nor could they be unambiguously placed geometrically. The two $MMo_4O_{13}\cdot 2H_2O$ were isostructural (space group $P-1$ no. 2) with each other.

Fig. 2 shows atomic configuration of asymmetric unit and atom-labeling scheme in $CoMo_4O_{13}\cdot 2H_2O$. According to the structural solution, every heavy-atom (Mo(1),(2) and Co(1)) was coordinated by six oxygen atoms, giving an octahedron. Bond valence sum (BVS) calculated for Co, Mo and O atoms of $CoMo_4O_{13}\cdot 2H_2O$ are given in Table 3. The BVS values confirmed that the Mo atoms were hexavalent and the Co atom was divalent. The very small BVS value of 0.30 at O(8) indicated that the O(8) atom was ascribed to OH_2, considering that hydrogen atoms were invisible in the present structural determination. Thus the $CoMo_4O_{13}\cdot 2H_2O$ structure is composed of three kinds of octahedra: $Co(1)O_6$, $Mo(1)O_6$, and $Mo(2)O_5OH_2$.

Fig. 3a shows a perspective view of the $CoMo_4O_{13}\cdot 2H_2O$ structure, illustrated in polyhedral representation. It was found that $CoMo_4O_{13}\cdot 2H_2O$ had an interesting pillared layer structure, in which molybdenum oxide (Mo-O) sheets were expanding in directions parallel to the crystallographic a–c plane. Fig. 3b shows a top view of the Mo-O sheet. This sheet is made up of infinite ribbons built up by corner-sharing of Z-shaped units consisting of two $Mo(1)O_6$ and two $Mo(2)O_5OH_2$ octahedra sharing edges. And the sheet has two kinds of penetration cavities: six-point star-shaped and diamond-shaped cavities. The planes shaded with declined lines, shown in Fig. 3b, of molybdenum octahedra are located on the top surface of the sheet. The same planes are also present on the bottom surface of the sheet. The three O atoms (O(1),(2),(7)), which are located on the shaded planes and are projecting into the six-point star-shaped cavity, coordinate to the Co(1) atom. The coordination of total six O atoms from two adjacent Mo-O sheets make up a $Co(1)O_6$ octahedra and build up the pillared layer structure of $CoMo_4O_{13}\cdot 2H_2O$.

3.3. Structural comparison between various tetramolybdates

Well-characterized tetramolybdates triclinic(t-) $K_2Mo_4O_{13}$ [15], orthorhombic(o-) $K_2Mo_4O_{13}$ [15], $Li_2Mo_4O_{13}$ (low- and high-temperature phases) [20,21], $Tl_2Mo_4O_{13}$ [22], $Cs_2Mo_4O_{13}$ [23], and $Ba(Sr)Mo_4O_{13}\cdot 2H_2O$ [24,25] are known. Their structures can be classified into five kinds of structures: one 3D, two 2D (layer) and two 1D (chain) ones. Except for the unusual structure of $Cs_2Mo_4O_{13}$, which is prepared by oxidizing melt of Cs_2CO_3/MoO_3/MoO_2 mixture, remaining four kinds of structures are made up of infinite ribbons built up by corner-sharing of Z-shaped units consisting of four MoO_n polyhedra sharing edges, and are formed in ordinary L/Mo/O (L = Li,K,Rb,Tl) melts or in hydrothermal solutions.

As for the structures prepared in hydrothermal solutions, three kinds of structures including the present pillared layer structure have been known. Fig. 4 shows the Mo-O frameworks in the structures. For $MMo_4O_{13}\cdot 2H_2O$ (M = Co,Ni), the molybdenum octahedra in the ribbon are all coplanar and lead to a straight ribbon similar to that of t-$K_2Mo_4O_{13}$. This ribbon is different from the twisted one of o-$K_2Mo_4O_{13}$ (or $Ba(Sr)Mo_4O_{13}\cdot 2H_2O$). In $MMo_4O_{13}\cdot 2H_2O$ the ribbons are linked one after another by corner-sharing of the $Mo(1)O_6$/$Mo(2)O_5OH_2$ sites to form the sheet structure, like for the ribbons consisting of MoO_6 and MoO_5 polyhedra in o-$K_2Mo_4O_{13}$ or $Ba(Sr)Mo_4O_{13}\cdot 2H_2O$. In t-$K_2Mo_4O_{13}$ the similar straight ribbons consisting of only regular MoO_6 octahedra are linked in pairs by edge-sharing to form the 1D chain. Thus the presence of OH_2 groups (i.e., $Mo(2)O_5OH_2$ octahedra) in the ribbon of $MMo_4O_{13}\cdot 2H_2O$ may be related to the corner-sharing linkage leading to the two-dimensional molybdenum-oxide (2D Mo-O) sheet. Such findings concerning the structural control into the layer (especially pillared layer) structures may give a key element for the synthesis of functionalized materials such as catalysts having a sterically restricted reaction field.

3.4. Thermal behavior of $MMo_4O_{13}\cdot 2H_2O$

TG-DTA of $CoMo_4O_{13}\cdot 2H_2O$ (Fig. 5) revealed a 5.35% weight loss occurring over the temperature range 423–573 K (Calc. for complete water loss = 5.25%). According to powder XRD results (Supplemental data Fig. S1), the structure of $CoMo_4O_{13}\cdot 2H_2O$ was

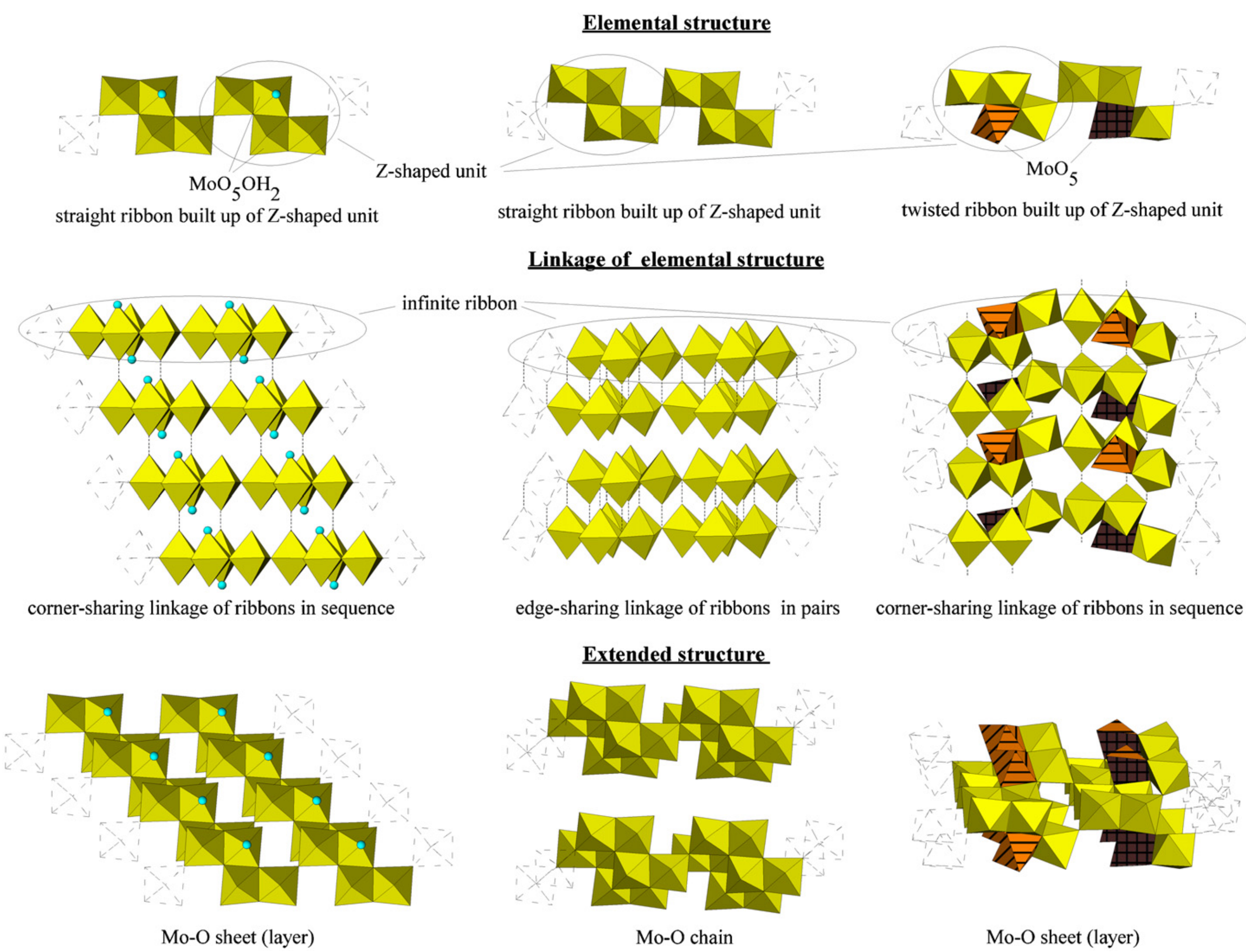

Fig. 4. Structural comparison among Mo-O frameworks of tetramolybdates prepared in hydrothermal solutions.

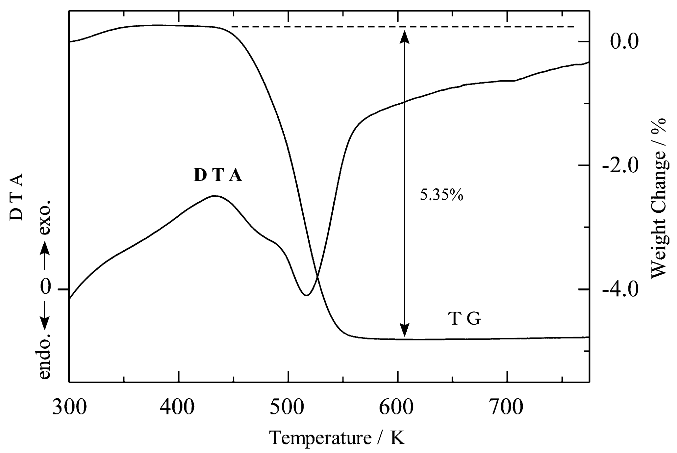

Fig. 5. TG-DTA curves in N_2 of $CoMo_4O_{13} \cdot 2H_2O$.

retained up to 423 K. The post-TG-DTA product heated to 573 K showed the XRD peaks due to MoO_3 and a new pattern unlike that of $CoMo_4O_{13} \cdot 2H_2O$, indicating decomposition of the pillared layer structure. The intensity ratio of the peaks of this pattern changed when the sample was heated to 773 K. This indicated that the pattern was probably due to a mixture. The pattern however could not be identified with any combinations of the patterns previously reported for the anhydrous cobalt molybdates, molybdenum oxides, and cobalt oxides. $NiMo_4O_{13} \cdot 2H_2O$ exhibited similar thermal behavior to that of $CoMo_4O_{13} \cdot 2H_2O$. The dehydration of $NiMo_4O_{13} \cdot 2H_2O$ occurred in a slightly higher temperature range 453–603 K than that for $CoMo_4O_{13} \cdot 2H_2O$.

These results indicated that the interesting pillared structure of MMo$_4$O$_{13} \cdot 2H_2O$ (M = Co,Ni) was not retained without the presence of the coordination water, but was stable up to 423 K for $CoMo_4O_{13} \cdot 2H_2O$ and 453 K for $NiMo_4O_{13} \cdot 2H_2O$.

Acknowledgment

The work at Kobe was supported by Grant-in-Aid for Scientific Research(C) 20550176, and the work at Binghamton was supported by the National Science Foundation under Grant DMR-0705657.

Appendix A. Supporting Information

Supplementary data associated with this article can be found in the online version at doi:10.1016/j.jssc.2008.10.001.

References

[1] A.P. Young, C.M. Schwartz, Science 141 (1963) 348.
[2] A.W. Sleight, B.L. Chamberland, Inorg. Chem. 7 (1968) 1672.
[3] K.T. Jacob, G.M. Kale, G.N.K. Iyengar, J. Mater. Sci. 22 (1987) 4274.
[4] M. Wiesmann, H. Ehrenberg, G. Wltschek, P. Zinn, H. Weitzel, H. Fuess, J. Magn. Magn. Mater. 150 (1995) L1.
[5] K.T. Jacob, S.V. Varamban, J. Alloys Compd. 280 (1998) 138.
[6] C. Livage, A. Hynaux, J. Marot, M. Nogues, G. Férey, J. Mater. Chem. 12 (2002) 1423.
[7] C. Mazzocchia, C. Aboumrad, C. Diagne, E. Tempesti, J.M. Herrmann, G. Thomas, Catal. Lett. 10 (1991) 181.
[8] J. Zou, G.L. Schrader, J. Catal. 161 (1996) 667.
[9] J.L. Brito, A.L. Barbosa, J. Catal. 171 (1997) 467.
[10] J.A. Rodriguez, S. Chaturvedi, J. Hanson, A. Albornoz, J.L. Brito, J. Phys. Chem. B 102 (1998) 1347.
[11] J.A. Rodriguez, S. Chaturvedi, J. Hanson, A. Albornoz, J.L. Brito, J. Phys. Chem. B 103 (1999) 770.
[12] K. Eda, Y. Uno, N. Nagai, N. Sotani, C. Chen, M.S. Whittingham, J. Solid State Chem. 179 (2006) 1453.
[13] K. Eda, Y. Uno, N. Nagai, N. Sotani, M.S. Whittingham, J. Solid State Chem. 178 (2005) 2791.
[14] K. Eda, K. Chin, N. Sotani, M.S. Whittingham, J. Solid State Chem. 178 (2005) 158.
[15] K. Eda, K. Chin, N. Sotani, M.S. Whittingham, J. Solid State Chem. 177 (2004) 916.
[16] K. Chin, K. Eda, N. Sotani, M.S. Whittingham, J. Solid State Chem. 164 (2002) 81.
[17] K. Eda, Y. Sato, Y. Iriki, Chem. Lett. 31 (2002) 952.
[18] [$CoMo_4O_{13} \cdot 2H_2O$] Calcd: Co 8.58 wt%, Mo 55.9 wt%, H_2O 5.25 wt%; found: Co 8.66 wt%, Mo 56.1 wt%, H_2O 5.35 wt%, IR: 3420(sh), 3375, 1600, 930(sh), 898, 776, 723, 598 cm^{-1}. [$NiMo_4O_{13} \cdot 2H_2O$] Calcd: Ni 8.55 wt%, Mo 55.9 wt%, H_2O 5.25 wt%; found: Co 8.45 wt%, Mo 55.6 wt%, H_2O 5.19 wt%, IR: 3420(sh), 3355, 1600, 936(sh), 907, 782, 728, 658(sh), 595 cm^{-1}.
[19] Spurious peaks and holes of residual electron density were observed in our structural determination. These may be due to poorness in overall quality of the diffraction data. Some crystals were subjected for the measurement, but no improvement could be obtained. The highest peak and deepest hole were located 1.01 Å from O1 and 0.83 Å from Mo1, respectively, for $CoMo_4O_{13} \cdot 2H_2O$, while those were located 1.10 Å from O1 and 0.87 Å from Mo2 for $NiMo_4O_{13} \cdot 2H_2O$. Powder diffraction patterns simulated using the present crystallographic data agreed well in peak positions with the observed ones (shown in Fig. 1), but disagreed in relative intensities. The differences in intensities may be due to a preferred orientation of the powder sample.
[20] B.M. Gatehouse, B.K. Miskin, J. Solid State Chem. 15 (1975) 274.
[21] B.M. Gatehouse, B.K. Miskin, J. Solid State Chem. 9 (1974) 247.
[22] P.P. Toledano, M. Touboul, Acta Cryst. B 34 (1978) 3547.
[23] J. Marrot, J.-M. Savariault, Acta Cryst. C 51 (1995) 2201.
[24] W.T.A. Harrison, Acta Cryst. C 55 (1999) 485.
[25] W.T.A. Harrison, L.L. Dussack, A.J. Jacobson, J. Solid State Chem. 116 (1995) 95.